Originally published in *Proceedings of the Fifth International Workshop on Compressible Turbulent Mixing*, ed. R. Young, J. Glimm & B. Boston.
ISBN 9810229100, World Scientific (1996).

Nonlinear Evolution of Multi–Mode Rayleigh–Taylor Instability in Two and Three Dimensions*

D. Shvarts[1,2], U. Alon[1,3], D. Ofer[1,2],
R. L. McCrory[2], and C. P. Verdon[2]

[1] Physics Department
Nuclear Research Center - Negev
P.O.B. 9001
Beer-Sheva, Israel

[2] Laboratory of Laser Energetics
University of Rochester
250 East River Rd.
Rochester NY 14623

[3] Physics of Complex Systems
The Weizmann Institute of Science
Rehovot, 76100, Israel

Abstract.
The nonlinear evolution of the Rayleigh-Taylor instability from multi-mode initial perturbations is studied using a modal model, in which nonlinear mode coupling and saturation are included in an equation for effective modes that describe the mixed region. The importance of mode coupling in the generation of large structure that dominates the late stage evolution, and the relative importance of long-wavelength components in the initial perturbation spectra on the late-stage evolution are studied. Multi-mode RT instability in three dimensions is also studied by both full-scale simulations and the modal model. The effect and late-stage memory loss of different aspect-ratios in the initial perturbation are demonstrated.

1 Introduction

The evolution of a multi-mode perturbation is quite different from the single mode case: instead of a periodic array of bubbles rising at a constant velocity, the late stage multi-mode bubble front penetration goes as $h \sim \alpha g t^2$, where $\alpha = 0.04 - 0.06$ [1, 5]. An inverse cascade occurs, by which larger and larger structure is continually generated [1]. The fundamental mechanism responsible for the inverse cascade in RT mixing fronts

*UA and DO thank the Laboratory of Laser Energetics for their hospitality and partial support. It is a pleasure to thank S.W. Haan, B.A. Remington, M. Rosen and D.H. Sharp for stimulating discussions.

is mode competition caused by the reduced drag of large structures. In the absence of a fixed single-mode periodicity, large structure expands and grows faster, sweeping smaller neighbors downstream. This large structures production mechanism may be viewed either as real-space bubble competition or wavenumber-space mode coupling and saturation. The multimode RT mixing process can therefore be studied using two, complementary, viewpoints: one approach, described elsewhere in this volume, utilizes single-mode bubble and spike evolution, together with two-bubble competition, as basic "particles" and "pair-interactions" in a non-equilibrium statistical-mechanics model of the mixing front [6, 2]; the other approach utilizes single-mode growth and saturation, together with two-mode couplings, to arrive at an evolution equation for effective modes that describe the mixed region. The modal approach is useful for predicting the evolution of complex initial perturbations. It is briefly described here and applied to RT mixing problems in 2 and 3 dimensions.

2 Modal model

The modal-model approach is based on analysis of the nonlinear coupling of modes that describe the front structure. The Fourier decomposition of the interface at early times is carried over to late times as a modal description of the mean mixing-zone structure. This approach was pioneered by S.W. Haan [7] who proposed a modal model of the mixing front, in which each of the initial modes grows exponentially with its linear growth rate, until a saturation amplitude is reached. After a mode reaches its saturation amplitude, its velocity is kept equal to the velocity at saturation. The saturation criterion for mode k, applicable for a multi-mode case, is that the root mean squared (RMS) amplitude of a narrow band near k (typically of order $0.1-0.5\ k$) reaches 0.1λ [7]. This is due to the constructive interference of nearby modes, which enhances the local structure size and causes earlier saturation than that of an isolated mode. As shown below, Haan's model adequately describes situations with a wide and continuous initial spectrum. However, in situations where the initial long-wavelength modes have only very small amplitudes, the inverse cascade is expected to correspond to long-wavelength modes generated by nonlinear couplings between the short-wavelength modes. We thus present a modal model that includes mode-coupling, which is an extension of Haan's model. Here we describe the model's essential features, while a detailed presentation is given in Ref [3]. The nonlinear interactions used are based on an equation of motion obtained by expanding the flow equations to second order in the mode amplitudes [8]

$$\begin{aligned}\ddot{Z}_k &= \gamma^2(k) Z_k \\ &\quad + Ak \sum_{k_2} [\ddot{Z}_{k_2} Z_{k_2'} (1 - \hat{k}_2 \cdot \hat{k}) + \dot{Z}_{k_2} \dot{Z}_{k_2'} (1/2 - \hat{k}_2 \cdot \hat{k} - 1/2 \hat{k}_2 \cdot \hat{k}_2')]\end{aligned} \tag{1}$$

where $\hat{k} = \mathbf{k}/k$ is a unit vector, $\mathbf{k}'_2 = \mathbf{k} - \mathbf{k}_2$ and $\gamma(k)$ is the linear growth-rate. This treats the first harmonic generation accurately, and all higher order couplings as combinations of two-mode couplings. This equation was employed in a recent work [8] to estimate the importance of mode-coupling in the early nonlinear stages. After the early nonlinear stages, however, Eq. (1) displays a fast divergence. In order to continue the analysis beyond the early stages, in the spirit of Haan's original model [9], the remaining nonlinear terms are effectively included in the present model through saturation to a constant velocity. This may be viewed as a form of nonlinear closure. A mode Z_k is saturated when $(\sum_{|k-k'|<0.25k} Z_{k'}^2)^{1/2} = 0.1 \cdot 2\pi/k$. For a mode with no close neighbors this equation reduces to saturation at 0.1λ. The mode's velocity is $\dot{Z}_k = \dot{Z}_k^{SAT}$ when $Z_k > Z_k^{SAT}$, where Z_k^{SAT} and $\dot{Z}_k^{SAT}$ are the mode's amplitude and velocity at saturation. The saturation applies both to modes in the initial spectrum, and to modes generated via mode-coupling. In the present model, after a mode has saturated, it ceases to participate in further mode-coupling. The phases of saturated modes may, however, change at late stages, when they correspond to harmonics of dominant long-wavelength modes. In this sense, the modes carry information relevant to the mixed zone structure at early stages, when the interface is more-or-less single valued, and at late stages when they represent either periodicities not much smaller than the dominant modes, or harmonics of these modes.

In order to demonstrate the effects of the initial perturbation and the importance of mode coupling in the instability evolution, we applied the model to initial spectra with varying amplitudes of long-wavelength components. The case of very small initial amplitudes, shown in Fig. 1, corresponds to the "classical" RT configuration [2, 8]. Thus, when all modes are still in their linear stage, the spectrum becomes dominated by the high-k modes around the wavenumber of maximum linear growth k_{max}. These modes later begin to generate low-k modes. In this case, the self-growth of the initial long-wavelength modes becomes negligible compared to their seeding by mode coupling. In Fig 1b, the mean wavenumber $\langle k \rangle$ and the standard deviation of the spectrum $\sigma = (\langle k^2 \rangle - \langle k \rangle^2)^{1/2}$ are plotted. The inverse cascade to low k's is seen. The spectrum width increases at early times due to the generation of harmonics of the initial modes, and at late times the spectrum approaches a scaled form with nearly constant σ/k. Haan's model [7] can not follow the mode-coupling induced inverse cascade in this case. On the other hand, when the low k modes have a large initial amplitude, at the time that mode coupling comes into play, they have already attained a significant amplitude through their own single mode growth. This case, shown in Fig. 2, may correspond to optimized ICF pellets, in which the acceleration time-scale is of the same order as the saturation times [8]. For this case, Haan's model [9] applies, and the spectrum cascade toward low k's is caused primarily by the sequential saturation of initial modes of increasing wavelength. We note that in both cases the bubble front penetration goes as $\alpha g t^2$, with $\alpha \approx 0.06$, suggesting that the dependence of α on the initial spectrum is not very

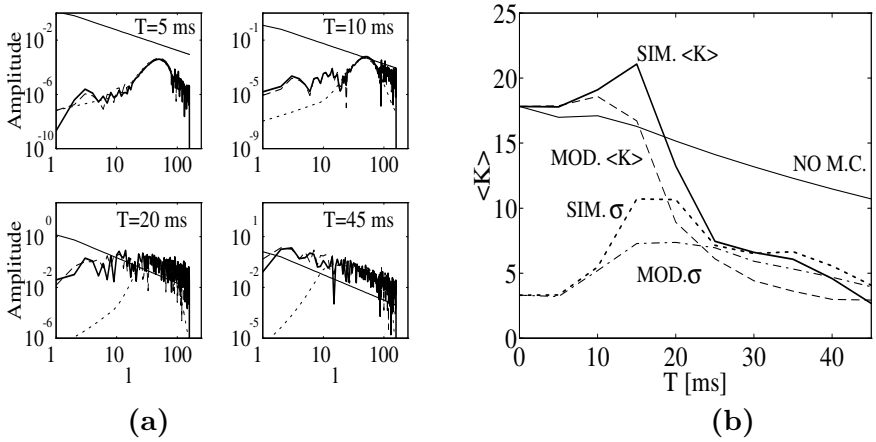

Figure 1: 2D "classical" configuration. The initial spectrum considered is of the form $|Z_k(0)/L^2| = \epsilon/(1+\eta(kL^2)$, where L is the domain width, and ϵ and η are dimensionless parameters. Here $\epsilon = 3e-20$ and $\eta = 1.5e-5$. The units used are typical of a rocket-rig experiment L = 9cm and $g = 3 \cdot 10^4\ cm/s^2$. (a) Spectra at $t = 5, 10, 20, 45\ ms$, simulation (bold full line), Haan's model (dotted line) and present model (dashed line), saturation amplitude (full line), (b) The mean wavenumber $\langle k \rangle$ (simulation- bold full line, present model - dashed line, Haan's model -full line), and the standard deviation of the spectrum.

strong.

3 3D Rayleigh-Taylor Instability

We now turn to the RT instability in 3D [10, 9]. Here we present preliminary results on the instability evolution in 3D from initial spectra with varying degrees of anisotropy. This complements studies that suggest that the initial anisotropy can affect the growth of single-mode initial perturbations [11, 14]. We performed numerical simulations of 3D RT mixing using LEEOR-3D [12], a 3D version of the 2D code used above. The simulated fluid region was of size $1 \times 1 \times 2$ with free-slip boundaries, with a resolution of $48 \times 48 \times 96$ cells. The interface between the fluids was at z=1, with A=1 and g=1. An initial velocity perturbation was imposed, as a sum of harmonic modes with random phases of ± 1 : $u = \sum u(k_x, k_y)$, where the z-component of $u(k_x, k_y)$ is $|u_z(k_x, k_y)| = u_0(k_x, k_y) cos(k_x x) cos(k_y y) exp(-k|z|)$ with $k = \sqrt{k_x^2 + k_y^2}$. We consider first an isotropic spectrum, where $u_0(k) = a_0 exp[-(k-k_0)^2/\sigma^2]$, i.e. a ring with a Gaussian cross-section in k-space. In the present example, $a_0 = 1e-3$, $k_0 = 8\pi$ and $\sigma = 2\pi$ were used. The vertically integrated heavy fluid volume fraction is plotted in

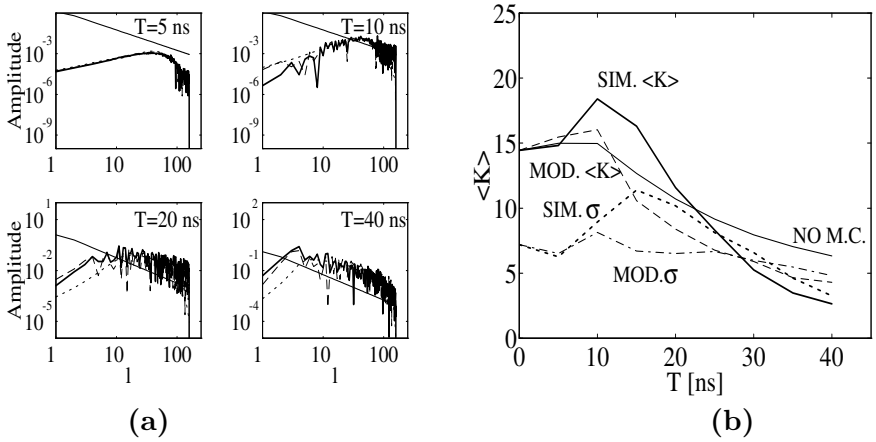

Figure 2: 2D ICF-like configuration, with initial spectrum parameters $\epsilon = 10^{-12}$ and $\eta = 1.5 \cdot 10^{-5}$. Units are typical of ICF applications, with $L = 900\ \mu m$ and $g = 3 \cdot 10^{15}\ cm/s^2$. (a) Spectra at $t = 5, 10, 20, 45\ ns$, simulation (bold full line), Haan's model (dotted line), present model (dashed line), saturation amplitude (full line). (b) $\langle k \rangle$ (simulation- bold full line, present model - dashed line, Haan's model -full line) and σ (simulation- bold dashed line, present model - dot-dashed line).

Fig. 3 at several times. It is seen that initially, the perturbation is composed of ridges of bubbles with contorted, worm-like shapes. These shapes have roughly the same mean characteristic size, but have widely varying orientations and aspect ratios. At first, these shapes grow in amplitude, and their tips become round. Bubble competition sets in at around $t = 2.0$, with the larger bubbles rising faster and overtaking their smaller neighbors. This is clearly seen in the smaller neighbors of the central bubble, which are swept down-stream at $t = 2.5 - 3.0$. Finally, the front is dominated by a few very large, rounded-tip bubbles. This illustrates a distinct 3D feature: the bubble shapes not only grow in size, but also tend to become round [14, 15, 13]. This is plausible on the basis of the principle that the structures seek the shape that minimizes the kinematic drag. We applied a 3D version of the modal-model described above to this case. The model spectra are shown in Fig 4(b). At early times the initial perturbation is seen, a ring in k-space. Gradually, the ring becomes noisy, due to the generation of modes via non-linear mode-coupling. Both short-wavelength (outside the ring) and long wavelength (inside the ring) modes are generated. The ring fills in towards $k_x = k_y = 0$ (at the center of the ring), corresponding to the generation of large structure. At late times, all traces of the initial ring are wiped out, and the spectrum becomes increasingly peaked towards lower k's.

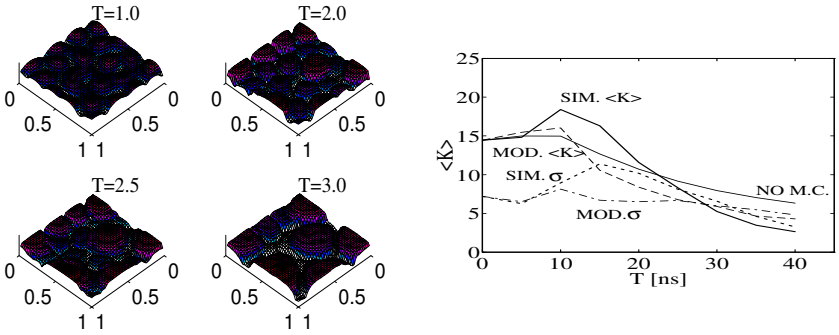

(a) **(b)**

Figure 3: 3D isotropic initial spectrum (ring). (a) Simulation results for the vertically integrated heavy fluid volume fraction at $t = 1, 2, 2.5, 3$ (b) Modal-model spectra. The point $k_x = k_y = 0$ is at the center of the ring.

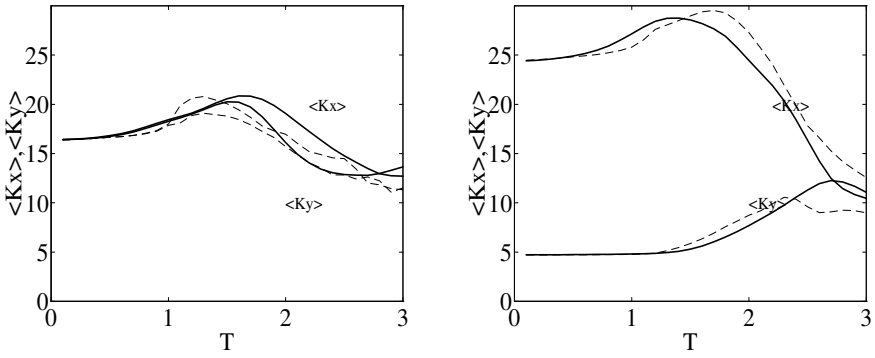

(a) **(b)**

Figure 4: $\langle k_x \rangle$ and $\langle k_y \rangle$: simulation (from spectrum of vertically integrated volume fraction) -bold full line, model- dashed line. (a) Isotropic case (Fig. 3), (b) Anisotropic case (Fig. 5)

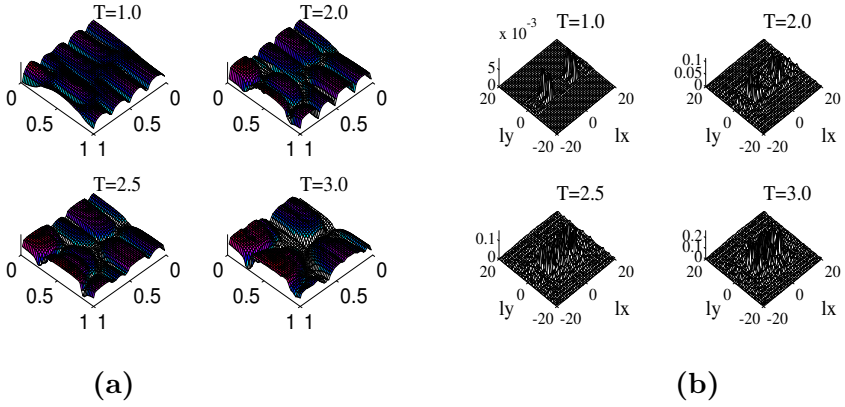

Figure 5: 3D anisotropic initial spectrum with $k_y = \pm 1,\ \pm 2$ only. (a) Simulation results for the vertically integrated heavy fluid volume fraction at $t = 1, 2, 2.5, 3$. (b) Modal-model spectra.

In order to quantitatively compare the model and the simulation, the first moments of the spectrum are plotted in Fig 4(a). The mean wavenumber $\langle k_x \rangle$ and $\langle k_y \rangle$ initially increase due to high-harmonic generation, and then decrease in time, due to the inverse cascade process. At all times the spectrum is nearly isotropic, and $\langle k_x \rangle \approx \langle k_y \rangle$. It is seen that the modal-model is in good agreement with the simulation results throughout the evolution.

We now consider the evolution of an initial perturbation that consists of a very anisotropic perturbation. The initial spectrum is a slice along the k_y axis of the above ring spectrum, containing modes with $k_y = \pm 1, \pm 2$ only. The interface from the simulation and the modal-model spectra are shown in Figs. 5(a)-(b). At early times, the interface is perturbed in the shape of long strips roughly parallel to the x axis. The small 3D perturbation, added by the modes with small k_y, introduces the long-wavelength ripples and modulations of these strips. At $t = 1.0$, elongated bubbles have formed, and most of the bubble competition is along the x-axis. The front behaves as a 2D front, with competition along only one direction. Competition along the y-axis begins only at late times. At the last time shown, $t = 3.0$, apart from traces of the y-axis modulation, the front resembles the previous isotropic front, composed of large, rounded bubbles. The initial anisotropy has been largely forgotten at late times. These effects are also clearly seen in the modal-model spectra shown in Fig. 5(b) and in Fig. 4(b).

References

[1] D.L. Youngs, Physica D 12,32 (1984).

[2] D. Shvarts, U. Alon, D. Ofer, R. L. McCrory, C.P. Verdon, Phys. Plas. 2,2466 (1995).

[3] D. Ofer, U. Alon, D. Shvarts, C.P. Verdon, R.L. McCrory, Phys. Plas. in press.

[4] D. Sharp, Physica D 12,3 (1984).

[5] C.L. Gardner, J. Glimm, O. McBryan, R. Menikoff, D.H. Sharp, Q. Zhang, Phys. Fluids 31,447 (1988); J. Glimm, X.R. Li, R. Menikoff, D.H. Sharp, Q. Zhang, Phys. Fluids A 2,2046 (1990).

[6] J. Glimm, D.H. Sharp, Phys. Rev. Lett. 64,2137 (1990); J. Glimm, Q. Zhang, D.H. Sharp, Phys. Fluids A 3,1333 (1991).

[7] S.W. Haan, Phys. Rev A 39,5812 (1989).

[8] S.W. Haan, Phys. Fluids B 3,2349 (1991).

[9] R.P.J. Town, A.R. Bell, Phys. Rev. Lett. 67,1863 (1990); K. Nishihara, H. Sakagami, Phys. Rev. Lett. 65,432 (1990).

[10] W. Manheimer, D. Colombant, E. Ott, Phys. Fluids 27,2164 (1984).

[11] J.W. Jacobs, I. Catton, J. Fluid. Mech. 187,329 (1988).

[12] J. Hecht, D. Ofer, U. Alon, D. Shvarts, S.A. Orszag, R.L. McCrory, Laser and Particle Beams 13,423 (1995).

[13] M.J. Dunning, S.W. Haan, "Analysis of weakly nonlinear 3D RT instability growth", UCRL-LR-105821-93-4, Lawrence Livermore National Laboratory, Livermore CA (1993), p. 179.

[14] J.P. Dahlburg, J.H. Gardner, G.D. Doolen, S.W. Haan, Phys. Fluids B 5,571 (1993).

[15] J. Hecht, U. Alon, D. Shvarts, Phys. Fluids 6,4019 (1994).